Orientational dynamics of the compressible nematic liquid crystals induced by a temperature gradient

A. V. Zakharov* and A. A. Vakulenko†

Saint Petersburg Institute for Machine Sciences, the Russian Academy of Sciences, Saint Petersburg 199178, Russia

(Received 5 August 2008; revised manuscript received 16 October 2008; published 23 January 2009)

We have carried out a numerical study of a system of hydrodynamic equations including director reorientation, fluid flow, temperature, and density redistribution across a compressible hybrid-oriented liquid crystal (HOLC) cell under the influence of a temperature gradient ∇T directed normal to the restricting surfaces, when the sample is heated both from below and above. Calculations show that under the influence of ∇T the compressible HOLC sample settles down to a stationary flow regime, both with the horizontal u and vertical w components of velocity $\mathbf{v}$, and u is directed in the opposite direction, approximately one order of magnitude less, than the one in the case of an incompressible HOLC cell. The role of hydrodynamic flow in the relaxation processes of the stress tensor components, for a number of dynamic regimes in the compressible HOLC cell containing 4-*n*-*pentyl*-4′-*cyanobiphenyl*, has been investigated.

DOI: 10.1103/PhysRevE.79.011708 PACS number(s): 61.30.Cz, 65.40.De

I. INTRODUCTION

Understanding how an elastic soft material, e.g., a liquid crystal, deforms under the influence of temperature gradient is a question of great fundamental interest, as well as an essential piece of knowledge in material science. In the field of liquid crystal (LC) phases, a great deal is known about their deformations under the influence of electric or magnetic fields [1], whereas comparatively little is known about the effect of temperature gradient on their static and dynamic properties.

For example, the seemingly simple problem of horizontal motion of a LC drop placed between two horizontal plates, and due to uniform heating from below, has attracted attention since the beginning of the 20th century [2]; on the other hand, some progress in understanding of the dynamical properties of both cholesteric and nematic LC drops under influence of a vertical temperature gradient, when the LC sample was heated from below, was achieved only in the past few years [3–11]. It has been shown that in the heat conduction regime the magnitude of the hydrodynamic flow v excited by the temperature gradient $\nabla T \sim \Delta T/d$ in the hybrid-oriented compressible LC (HOCLC) cell, with thickness d, is proportional to $v \sim \frac{d}{\eta}\sigma_{zx}^{tm}$, where $\Delta T = T_2 - T_1 > 0$ (the range $[T_2, T_1]$ falls within the stability region of the nematic phase) is the temperature difference on the LC cell boundaries, η is the viscosity, and $\sigma_{zx}^{tm} \sim \xi\frac{\Delta T}{d^2}$ is the tangential component of the thermomechanical stress tensor σ_{ij}^{tm}, and ξ is the thermomechanical constant. In the direction of the hydrodynamic flow $\mathbf{v}$ influences both the direction of the heat flow and the character of the preferred anchoring of the average molecular direction $\hat{\mathbf{n}}$ to the restricted surfaces [9,10]. Measurements of the temperature-induced flow have been performed on the HOCLC cell [7], where the material exposed by the vertical temperature gradient was fixed to solid substrates, for instance, the planar to the upper and homeotropically to the lower restricted surfaces. The main result of these experimental studies [7,8] is the estimate of the thermomechanical constant $\xi \sim 10^{-12}$ J/K m based on the measurements of the liquid crystal flow in the horizontal direction. Despite the fact that certain quantitative advances in the hydrodynamical description of confined nematic LCs under the influence of the temperature gradient have been achieved only for the case of incompressible fluids [9], it is still too early to talk about the development of a theory which would make it possible to describe the relaxation process in the case of compressible nematic LCs. In an attempt to make the next step towards the theoretical description of dissipation processes in confined compressible LCs under the influence of a temperature gradient, we have performed a numerical study of the system of hydrodynamic equations that include both director motion and flow of compressible fluid, as well as the redistribution of the temperature and density fields. To calculate it, one must include the equation of state, the equation for the velocity $\mathbf{v}$, and consider the coupled director-velocity equations in the framework of the well-established Ericksen-Leslie theory [12,13], as well as the thermoconductivity equation for the temperature field $T(\mathbf{r},t)$ [14].

The outline of this paper is as follow. The system of hydrodynamic equations describing both director motion and fluid flow of a compressible liquid crystal phase confined between two bounding surfaces, with accounting for the heat conduction, caused by heating from below or above, is given in Sec. II. Numerical results for the relaxation regimes, caused by the vertical temperature gradient, describing orientational relaxation of the director, velocity, and temperature, as well as the stress tensor components are given in Sec. III and IV. Conclusions are summarized in Sec. V.

II. FORMULATION OF THE BALANCE OF THE MOMENTUM AND TORQUE EQUATIONS AND CONDUCTIVITY EQUATION FOR COMPRESSIBLE NEMATIC FLUIDS

Upon assuming a compressible fluid $\partial_t\rho + \nabla\cdot(\rho\mathbf{v}) = 0$, the hydrodynamic equations describing the reorientation of the

*Author to whom correspondence should be addressed. avz02@yahoo.com; www.ipme.ru/-zakharov

†avak@microm.ipme.ru; www.ipme.ru/-vakulenko

LC phase confined between two solid surfaces, when a horizontal LC layer heated both from below or above, can be derived from the balance of elastic, viscous, and thermomechanical torques $\mathbf{T}_{\rm el}+\mathbf{T}_{\rm vis}+\mathbf{T}_{\rm tm}=0$, the Navier-Stokes equation for the velocity field $\mathbf{v}$, excited by the temperature gradient ∇T, and the equation for the heat conduction. We consider a LC system composed of asymmetric polar molecules, such as *cyanobiphenyls*, the density ρ, which are confined between two solid surfaces that impose a preferred orientation of the average molecular direction $\hat{\mathbf{n}}(\mathbf{r})$ on the bounding surfaces, for instance, homeotropic on the lower and planar on the upper bounding surfaces. So, one deals with the HOCLC cell under influence of the temperature gradient ∇T directed parallel to the unit vector $\hat{\mathbf{k}}$. Here $\hat{\mathbf{k}}$ is a unit vector directed away from the lower substrate to the upper one. The coordinate system defined by our task assumes that the director $\hat{\mathbf{n}}(t,\mathbf{r})$ is in the xz plane (or in the yz plane), where $\hat{\mathbf{i}}$ is the unit vector directed parallel to the bounding surfaces, which coincides with the planar director orientation, for instance, on the upper bounding surface $(\hat{\mathbf{i}}\|\hat{\mathbf{n}}_{z=d})$, and $\hat{\mathbf{j}}=\hat{\mathbf{k}}\times\hat{\mathbf{i}}$. Assuming that the temperature gradient ∇T varies only in the z direction, $\nabla T=\frac{\partial T(z,t)}{\partial z}\hat{\mathbf{k}}$, we can suppose that the components of the director $\hat{\mathbf{n}}=\sin\theta(t,z)\hat{\mathbf{i}}+\cos\theta(t,z)\hat{\mathbf{k}}$, as well as the rest of the physical quantities also depend only on the z coordinate. Here θ denotes the polar angle, i.e., the angle between the direction of the director $\hat{\mathbf{n}}$ and the normal $\hat{\mathbf{k}}$ to the boundary surfaces. If the director is disturbed by the heat flow, the relaxation of $\hat{\mathbf{n}}(t,z)$ to its equilibrium orientation $\hat{\mathbf{n}}_{\rm eq}(z)$ in the HOCLC cell, is governed by elastic $\mathbf{T}_{\rm el}$, viscous $\mathbf{T}_{\rm vis}$, and thermomechanical $\mathbf{T}_{\rm tm}$ torques exerted per unit LCs volume. Note that the horizontal LC layer, being initially at rest, if heated both from below or above, starts moving in the horizontal direction, due to the temperature gradient [7–9]. This gradient, if expressed in suitable dimensionless units, is called the Rayleigh (R) number. As long as the Rayleigh number is not too large, the heat is transported by conduction [14]. It should be pointed out that a thin horizontal layer of quiescent LC fluid heated from below becomes unstable to convection via the Rayleigh-Benard mechanism. The instability occurs at value $R=R_c\sim 1708$, independent of the fluid under consideration [15]. Taking into account that the size of the LC cell $\sim 10-20$ μm, in our case [9] $R\ll R_c$, and the driving force is not strong enough to set up of convection via the Rayleigh-Benard mechanism: thus, in the following we are focused primarily on the heat conduction regime in the HOLCC [9]. Note that any physical effect that reorients the director also induces an additional flow in the LC phase, which, in turn, is coupled to the director [1]. In the following one deals with the complicated flow $\mathbf{v}(t,z)=v_x(t,z)\hat{\mathbf{i}}+v_z(t,z)\hat{\mathbf{k}}=u(t,z)\hat{\mathbf{i}}+w(t,z)\hat{\mathbf{k}}$ excited by the temperature gradient and the director reorientation. In the case of the quasi-two-dimensional compressible LC system, where the molecules of the HOCLC cell align and tilt relative to the normal $\hat{\mathbf{k}}$, and thereby define an array of unit vectors $\hat{\mathbf{a}}_i$ in the plane $x-z$ of the HOCLC cell, the dimensionless compressibility condition and the torque balance equation describing the reorientation of the LC phase can be written as [9]

$$\rho_\tau+(\rho w)_z=0, \tag{1}$$

$$\bar{\gamma}_1(\chi)\theta_\tau=\mathcal{A}(\theta)u_z+[\mathcal{G}(\theta)\theta_z]_z-\frac{1}{2}\mathcal{G}_\theta(\theta)\theta_z^2-\delta_1\chi_z\theta_z\left(\frac{1}{2}+\sin^2\theta\right), \tag{2}$$

where $\rho\equiv\rho(\tau,z)=\rho(\tau,z)/\rho_0$ is the dimensionless density, ρ_0 is the mass density of the LC phase, $\rho_\tau=\partial\rho(\tau,z)/\partial\tau$, $u_z=\partial u(\tau,z)/\partial z$, $w_z=\partial w(\tau,z)/\partial z$, $\mathcal{A}(\theta)=\bar{\mathcal{A}}(\theta)/\gamma_{10}=\frac{1}{2}[\gamma_1(\chi)-\gamma_2(\chi)\cos 2\theta]/\gamma_{10}$, $\mathcal{G}(\theta)=[K_1(\chi)\sin^2\theta+K_3(\chi)\cos^2\theta)/K_{10}$, $\mathcal{G}_\theta(\theta)$ is the derivative of $\mathcal{G}(\theta)$ with respect to θ, $\theta_z=\partial\theta(\tau,z)/\partial z$, $\chi_z=\partial\chi(\tau,z)/\partial z$, $\chi(\tau,z)=T(\tau,z)/T_{NI}$ is the dimensionless temperature, T_{NI} is the nematic-isotropic transition temperature, $\gamma_1(\chi)$ and $\gamma_2(\chi)$ are the temperature-dependent rotational viscosity coefficients (RVCs), $K_1(\chi)$ and $K_3(\chi)$ are the splay and bend elastic constants of the LC phase, $\bar{\gamma}_1(\chi)=\gamma_1(\chi)/\gamma_{10}$, and γ_{10} and K_{10} are the highest values of the RVC $\gamma_1(\chi)$ and the splay constant $K_1(\chi)$ in the temperature interval $[\chi_1,\chi_2]$ belonging to the nematic phase. Here $\tau=(K_{10}/\gamma_{10}d^2)t$ is the dimensionless time, $\bar{z}=z/d$ is the dimensionless distance away from the lower solid surface, $\delta_1=\xi T_{NI}/K_{10}$ is the parameter of the system, and $\xi\sim 10^{-12}$ J/mK is the thermomechanical constant [7]. Notice that the overbars in the space variable z have been eliminated. In the case of compressible fluid the dimensionless Navier-Stokes equation reduces to [9]

$$\delta_2\rho\frac{dw(\tau,z)}{d\tau}=\partial_z\sigma_{zz}, \tag{3}$$

$$\delta_2\rho\frac{du(\tau,z)}{d\tau}=\partial_z\sigma_{zx}, \tag{4}$$

where $\sigma_{zi}=\sigma_{zi}^v+\sigma_{zi}^e$ $(i=x,z)$ are both the shear and normal stress tensor components, $\sigma_{zx}^v(\tau)=\frac{\delta\mathcal{R}(\tau)}{\delta u_z}$ and $\sigma_{zz}^v(\tau)=\frac{\delta\mathcal{R}(\tau)}{\delta w_z}$ are the viscous contributions to these stress tensor components, $\mathcal{R}(\tau,z)=\frac{\gamma_{10}d^4}{K_{10}^2}\mathcal{R}(t,z)$ is the full dimensionless Rayleigh dissipation function, where $\mathcal{R}(t,z)=\mathcal{R}_{\rm vis}+\mathcal{R}_{\rm tm}+\mathcal{R}_{\rm th}$, and $\mathcal{R}_{\rm vis}=\frac{1}{2}h(\theta)u_z^2-\bar{\mathcal{A}}(\theta)\theta_t u_z+\frac{1}{2}\gamma_1\theta_t^2+\frac{\beta_0}{6}u_z w_z\sin 2\theta+(\frac{\beta_0}{18}+\frac{1}{2}\xi_v)w_z^2$ is the viscous contribution, $\mathcal{R}_{\rm tm}=\xi\theta_t\theta_z T_z(\frac{1}{2}+\sin^2\theta)-\frac{3}{2}\xi T_z u_z\theta_z\sin^2\theta-\frac{\xi}{4}T_z w_z\theta_z\sin 2\theta$ is the thermomechanical contribution, and $\mathcal{R}_{\rm th}=\frac{1}{2T}(\lambda_\parallel\cos^2\theta+\lambda_\perp\sin^2\theta)T_z^2$ is the thermal contribution, respectively, whereas $\sigma_{zz}^e=-\bar{\mathcal{G}}(\theta)\theta_z^2=-2W_F$ and $\sigma_{zx}^e=0$ (see the Appendix) are the elastic contributions to the normal and shear components of the stress tensor. Here $h(\theta)=\alpha_1(T)\sin^2\theta\cos^2\theta-\bar{\mathcal{A}}(\theta)(\theta)\theta_t u_z+\frac{1}{2}\alpha_4(T)+g(\theta)$, $g(\theta)=\frac{1}{2}[\alpha_6(T)\sin^2\theta+\alpha_5(T)\cos^2\theta)$, $T_z=\partial T(t,z)/\partial z$, $\beta_0=\alpha_1+\alpha_5+\alpha_6+\frac{3}{2}\alpha_4$, $\delta_2=\rho_0K_{10}/\gamma_{10}^2$ is a parameter of the system, and ξ_v is the volume viscosity. Here $\alpha_i(T)$ $(i=1,\ldots,6)$ are the temperature-dependent six Leslie coefficients, $\lambda_\parallel$ and $\lambda_\perp$ are the heat conductivity coefficients parallel and perpendicular to the director $\hat{\mathbf{n}}$. Note, that in the case of very thin LC layer the hydrostatic pressure gradient ∇P contribution both to Eqs. (3) and (4) are equal to zero. Now the full dimensionless stress tensor components σ_{zz} and

σ_{zx} are given by [9] $\sigma_{zz}(\tau)=\frac{\bar{\beta}_0}{6}u_z \sin 2\theta+(\frac{\bar{\beta}_0}{9}+\xi_v)w_z - \frac{\delta_1}{4}\chi_z\theta_z \sin 2\theta-\mathcal{G}(\theta)\theta_z^2$ for the normal component and $\sigma_{zx}(\tau)=\bar{h}(\theta)u_z-\mathcal{A}(\theta)\theta_\tau-\frac{3}{2}\delta_1\chi_z\theta_z \sin^2\theta+\frac{\bar{\beta}_0}{6}w_z \sin 2\theta$ for the shear component, where $\bar{h}(\theta)=h(\theta)/\gamma_{10}$ and $\bar{\beta}_0=\beta_0/\gamma_{10}$. When the small temperature gradient ∇T (~ 0.05 [K/μm]) is set up across the HOCLC cell, we expect that the temperature field $T(t,z)$ satisfies the heat conduction equation [14]

$$\rho C_p \frac{dT}{dt} = -q_{z,z}, \tag{5}$$

where C_p is the heat capacity and $q_z=-T\frac{\delta\mathcal{R}}{\delta T_z}$ is the heat flow in the HOCLC cell. Taking into account both that $\mathbf{v}=u(t,z)\hat{\mathbf{i}}+w(t,z)\hat{\mathbf{k}}$ and $\hat{\mathbf{n}}=(\sin\theta,0,\cos\theta)$, the last equation can be rewritten in the dimension form [9] as

$$\rho C_p \frac{dT}{dt} = \lambda_\perp[T_z(\lambda\cos^2\theta+\sin^2\theta)]_z+\xi\left\{\theta_z T\left[\theta_t\left(\frac{1}{2}+\sin^2\theta\right)-\frac{3}{2}u_z\sin^2\theta\right]\right\}_z-\frac{\xi}{4}[Tw_z\theta_z\sin 2\theta]_z, \tag{6}$$

where $\lambda=\lambda_\parallel/\lambda_\perp$.

Notes that the density ρ, pressure P, and the temperature T of the liquid-crystal system are connected by an equation of state, which in our case takes the form ("Boussinesq approximation") [16]

$$\rho=\rho_0[1-\alpha(T-T_1)], \tag{7}$$

where $\alpha=\frac{1}{\rho}(\frac{\partial\rho}{\partial T})_P$ is the volume expansion coefficient. Taking into account the last equation, the compressibility condition can be rewritten in the dimensionless form as

$$-\chi_\tau-\chi_z w-(\chi-\chi_1)w_z+\frac{1}{\delta_5}w_z=0, \tag{8}$$

whereas both Eqs. (3) and (4) takes the forms

$$\delta_2\{[1-\delta_5(\chi-\chi_1)]\}\frac{dw}{d\tau}=\left[\bar{h}(\theta)u_z-\mathcal{A}(\theta)\theta_\tau-\delta_1\chi_z\theta_z\sin^2\theta+\frac{\bar{\beta}_0}{6}w_z\sin 2\theta\right]_z \tag{9}$$

and

$$\delta_2\{[1-\delta_5(\chi-\chi_1)]\}\frac{du}{d\tau}=\left[\frac{\bar{\beta}_0}{6}\left(u_z\sin 2\theta+\frac{2}{3}w_z\right)+\xi_v w_z-\frac{\delta_1}{4}\chi_z\theta_z\sin 2\theta-\mathcal{G}(\theta)\theta_z^2\right]_z, \tag{10}$$

respectively. Here $\delta_5=T_{\mathrm{NI}}\alpha$ is the parameter of the system. We also expect that the dimensionless temperature field $\chi(\tau,z)$ satisfies the heat conduction equation [9]

$$\delta_3\{[1-\delta_5(\chi-\chi_1)]\}\frac{d\chi}{d\tau}=[\chi_z(\lambda\cos^2\theta+\sin^2\theta)]_z+\delta_4\left\{\chi\theta_z\left[\theta_\tau\left(\frac{1}{2}+\sin^2\theta\right)-\frac{3}{2}u_z\sin^2\theta\right]-\frac{1}{4}w_z\sin 2\theta\right\}_z, \tag{11}$$

where $\delta_3=\rho_0 C_p K_{10}/(\gamma_{10}\lambda_\perp)$ and $\delta_4=T_{\mathrm{NI}}K_{10}\xi/(\gamma_{10}\lambda_\perp d^2)$ are extra two parameters of the system. Note that the overbars in the space variable z, in the last four Eqs. (8)–(11) have also been eliminated.

Consider now the LC film confined between two solid surfaces when the director $\hat{\mathbf{n}}$ is strongly anchored to both planes, homeotropically to the lower and planar to the upper bounding surfaces

$$\theta(z)_{z=0}=0, \quad \theta(z)_{z=1}=\frac{\pi}{2}, \tag{12}$$

and its initial orientation is perturbed to be tilted with respect to the interface, with $\theta(\tau=0,0.0<z\leqslant 1.0)=\frac{\pi}{2}$, and then allowed to relax to its equilibrium value $\theta_{\mathrm{eq}}(z)$. The velocity on these surfaces has to satisfy the no-slip boundary condition

$$u(z)_{z=0}=0, \quad u(z)_{z=1}=0,$$

$$w(z)_{z=0}=0, \quad w(z)_{z=1}=0. \tag{13}$$

On the other hand, when the director $\hat{\mathbf{n}}$ is strongly anchored to the lower and weakly to the upper bounding surface, so the anchoring energy takes the form [1] $W=\frac{1}{2}A\sin^2(\theta_s-\theta_0)$, where A is the anchoring strength, θ_s and θ_0 are the polar angles corresponding to the director orientation on the upper bounding surface $\hat{\mathbf{n}}_s$ and easy axis $\hat{\mathbf{e}}$, the torque balance transmitted to the upper surface entails that the director angle has to satisfy the boundary conditions

$$\theta(z)_{z=0}=0,$$

$$[\partial\theta(z)/\partial z]_{z=1}=\frac{Ad}{2K_{30}}\sin 2\Delta\theta, \tag{14}$$

where $\Delta\theta=\theta_s-\theta_0$, whereas the initial orientation of the director is disturbed to be tilted with respect to the interface, with $\theta(\tau=0,0.0<z\leqslant 1.0)=\frac{\pi}{2}$, and then allowed to relax to its equilibrium value $\theta_{\mathrm{eq}}(z)$.

Now, the reorientation of the director in the LC film confined between two solid surfaces, when the relaxation regime is governed by the viscous, elastic, and thermomechanical forces, and with accounting for the flow, can be obtained by solving the system of the nonlinear partial differential Eqs. (2) and (8)–(11), with the appropriate boundary and initial conditions $\theta(0,0.0<z\leqslant 1.0)=\frac{\pi}{2}$, both for the polar angle $\theta(\tau,z)$ [Eqs. (12) and (14)] and the velocities $u(\tau,z)$ and $w(\tau,z)$ [Eq. (13)].

For the case of 4-*n*-*pentyl*-4′-*cyanobiphenyl* (5CB), at temperature corresponding to nematic phase, the mass density $\sim 10^3$ kg/m^3, $T_{\mathrm{NI}}(5\mathrm{CB})\sim 307$ K, the experimental data

for elastic constants [17] $K_1(T)$ and $K_3(T)$ vary between 5 and 13 pN, and 8 and 19 pN, respectively, whereas the experimental data for $\gamma_1(T)$, obtained using different experimental techniques, vary between 0.033 and 0.071 Pa s [18]. So, the highest values are $K_{10} \sim 13$ pN, $K_{30} \sim 19$ pN, and $\gamma_{10} \sim 0.071$ Pa s, respectively. The experimental values of A vary between 10^{-4} and 10^{-6} J/m^2 [19]. In the following, we use the measured values, obtained by the adiabatic screening calorimetry and photopyroelectric techniques, both for the specific heat $C_p \sim 10^3$ J/kg K [20], and the thermal conductivity coefficients $\lambda_{\parallel} \sim 0.24$ and $\lambda_{\perp} \sim 0.13$ W/mK [21], the calculated value of the thermomechanical constant $\xi \sim 10^{-12}$ J/mK [7], measured values of the Leslie coefficients $\alpha_i(T)$ $(i=1,\ldots,6)$ [18], and the values of the volume expansion $\alpha \sim 10^{-3}$ K^{-1} [22], and the volume viscosity $\xi_v = 0.2$ Pa s coefficients, respectively. In the case of planar alignment on the upper surface, when the polar angles θ_s and θ_0 are both close to $\frac{\pi}{2}$, $\Delta\theta$ is small, $\Delta\theta \sim 1-3°$, and therefore $\sin 2\Delta\theta \sim 2\Delta\theta$, so the combination of $(Ad/K_{30})\Delta\theta$ values is approximately 0.1. The set of parameters values, which are involved in Eqs. (2) and (8)–(11), are thus $\delta_1 \sim 24$, $\delta_2 \sim 2 \times 10^{-6}$, $\delta_3 \sim 6 \times 10^{-4}$, $\delta_4 \sim 2 \times 10^{-9}$, and $\delta_5 \sim 0.3$. Using the fact that $\delta_2 \ll 1$, the Navier-Stokes equations (9) and (10) can be considerably simplified as velocities follows adiabatically the motion of the director. Thus, the whole left-hand side of Eqs. (9) and (10), can be neglected, reducing it to

$$\sigma_{zx} = \bar{h}(\theta)u_z - \mathcal{A}(\theta)\theta_\tau - \frac{3}{2}\delta_1\chi_z\theta_z \sin^2\theta + \frac{\bar{\beta}_0}{6}w_z \sin 2\theta = \mathcal{C}_1(\tau) \tag{15}$$

and

$$\sigma_{zz} = \frac{\bar{\beta}_0}{6}\left(u_z \sin 2\theta + \frac{2}{3}w_z\right) + \xi_v w_z - \frac{\delta_1}{4}\chi_z\theta_z \sin 2\theta - \mathcal{G}(\theta)\theta_z^2 = \mathcal{C}_2(\tau), \tag{16}$$

respectively, where the functions $\mathcal{C}_1(\tau)$ and $\mathcal{C}_2(\tau)$ does not depends on z and will be fixed by the boundary condition (14). Equation (11) also can be considerably simplified, because both parameters δ_3 and $\delta_4 \ll 1$, and the whole left-hand side of Eq. (11), as well as the second term, can be neglected so that Eq. (11) becomes

$$[\chi_z(\lambda \cos^2\theta + \sin^2\theta)]_z = 0. \tag{17}$$

The last equation has a solution

$$\chi(\tau,z) = \frac{\Delta\chi}{I}\int_0^z (\lambda \cos^2\theta + \sin^2\theta)^{-1}dz + \chi_i, \tag{18}$$

where $I = \int_0^1 (\lambda \cos^2\theta + \sin^2\theta)^{-1}dz$, $\Delta\chi = (T_2 - T_1)/T_{NI}$, and $\chi_i = T_i/T_{NI}$, and $T_i = T_1$ or T_2, respectively.

III. ORIENTATIONAL RELAXATION OF THE DIRECTOR, VELOCITY, AND TEMPERATURE FIELDS IN THE HOCLC CELL

The relaxation of the director $\hat{\mathbf{n}}$ to its equilibrium orientation $\hat{\mathbf{n}}_{eq}$, which is described by the polar angle $\theta(\tau,z)$, from the initial condition $\theta(\tau=0, 0.0 < z \leqslant 1.0) = \frac{\pi}{2}$ to θ_{eq} [see, Fig. 1(b)], and both velocities $u(\tau,z) = v_x(\tau,z)$ and $w(\tau,z) = v_z(\tau,z)$ [see Figs. 1(a) and 1(c)], in the HOCLC cell, at different times $(\tau(1) = 0.1$ (~7 s) [curve (1)],..., $\tau(5) = \tau_R = 0.5$ (~36 s) [curve (5)]), are shown in Fig. 1. In the studied case, the sample is heated from above with the dimensionless temperature difference $\Delta\chi = 0.0162$ (~5 K). This has been calculated by solving of the system of the nonlinear partial differential equations (2), (8)–(10), and (18), together with the boundary conditions (12) and (13), by means of the numerical relaxation method [23]. Here τ_R is the relaxation time of the system. In that case, the lower cooler surface was kept $\chi_{z=0} = \chi_1 = 0.97$ ($T_1 \sim 298$ K). The relaxation processes both of the dimensionless temperature $\chi(\tau,z)$ and density $\rho(\tau,z)$ to their equilibrium distributions $\chi_{eq}(z)$ and $\rho_{eq}(z)$ across the LC cell, are characterized practically the linear increasing the values of $\chi(\tau,z)$, from χ_1 to χ_2 [see Fig. 2(a)], and decreasing the values of $\rho(\tau,z)$, from $\rho(z=0)$ to $\rho(z=1)$ [see Fig. 2(b)], respectively. In the calculations, the re-

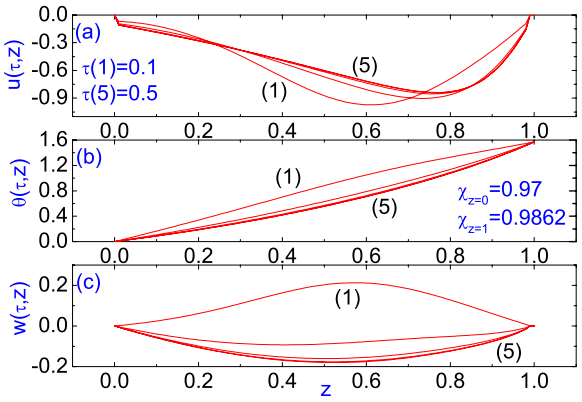

FIG. 1. (Color online) The velocity components $v_x(\tau,z)$ (a) and $v_z(\tau,z)$ (c), as well as the polar angle $\theta(\tau,z)$ [in rad] (b) [$\tau = (K_{10}/\gamma_{10}d^2)t$ is a dimensionless time] vs distance z away from the lower cooler ($\chi_{z=0} = \chi_1 = 0.97$) to the upper warmer ($\chi_{z=1} = \chi_1 + \Delta\chi$) bounding surfaces at different times $\tau(1) = 0.1$ [curve (1)] and $\tau(k) = (k/5)\tau_R$, $k = 1,\ldots,5$, whose values increase from curve (1) to curve (5). Here $\Delta\chi = 0.0162$ and $\tau_R \sim 0.5$.

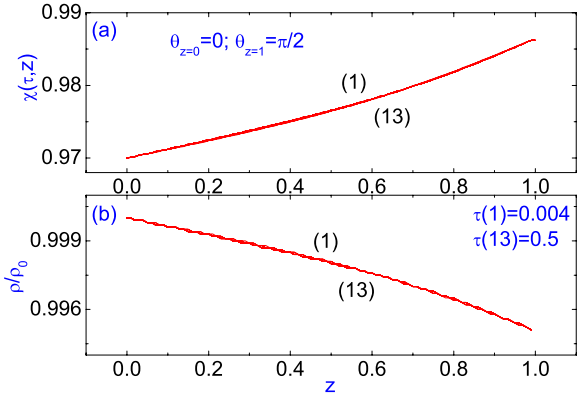

FIG. 2. (Color online) The dimensionless temperature $\chi(\tau,z)$ (a) and density $\rho(\tau,z)$ (b) vs distance z away from the lower cooler ($\chi_{z=0} = \chi_1 = 0.97$) to the upper warmer ($\chi_{z=1} = \chi_1 + \Delta\chi$) bounding surfaces during the time term τ_R corresponding to $\Delta\chi$ as in Fig. 1.

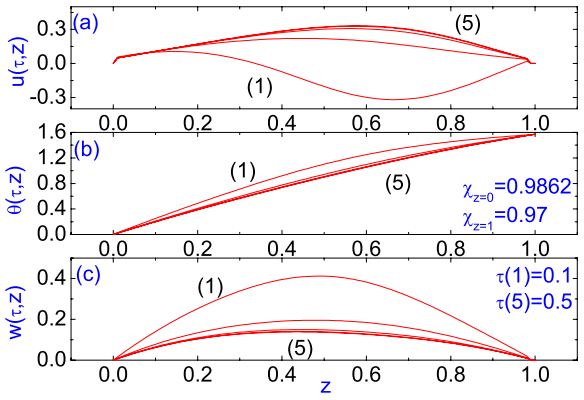

FIG. 3. (Color online) The same as in Fig. 1, but the temperature gradient directed from the upper cooler ($\chi_{z=1}=\chi_2=0.97$) to the lower warmer ($\chi_{z=0}=\chi_2+\Delta\chi$) bounding surfaces during the time term $\tau_R\sim 0.5$. Here $\Delta\chi=0.0162$.

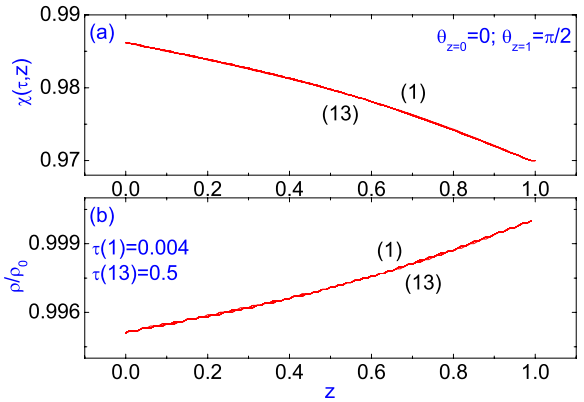

FIG. 4. (Color online) The same as in Fig. 2, but the temperature gradient directed from the upper cooler ($\chi_{z=1}=\chi_2=0.97$) to the lower warmer ($\chi_{z=0}=\chi_2+\Delta\chi$) bounding surfaces during the time term $\tau_R\sim 0.5$. Here $\Delta\chi=0.0162$.

laxation criterion $\epsilon=|(\theta_{(m+1)}(\tau,z)-\theta_{(m)}(\tau,z))/\theta_{(m)}(\tau,z)|$ was chosen equal to be 10^{-4}, and the numerical procedure was then carried out until a prescribed accuracy was achieved. Here m is the iteration number and τ_R is the relaxation time. According to our calculations, the relaxation processes both the dimensionless velocities $v_x(\tau,z)$ and $v_z(\tau,z)$, in the HOCLC cell, are characterized by the monotonic decrease of $|v_i(\tau,z)|$ $(i=x,z)$ upon increasing τ, before getting to the equilibrium distributions $u_{\rm eq}(z)$ and $w_{\rm eq}(z)$ across the LC cell. These distributions are characterized by the minimums near the middle part of the LC cell, where both the hydrodynamic flows are directed in the negative direction [see Figs. 1(a) and 1(c)]. Notes that the vertical component of the hydrodynamic flow $w(\tau,z)$ change a direction, from the positive to the negative, across the full thickness of the LC cell, after the time term $\Delta\tau\sim 0.2$ ($\sim$14 s), from the beginning of the relaxation process, whereas the horizontal component of the hydrodynamic flow $u(\tau,z)$ is keep a negative direction during the full relaxation term $\tau_R\sim 0.5$ ($\sim$36 s). The maximum both the absolute magnitudes of the dimensionless velocities $v_i(\tau,z)=(\gamma_{10}d/K_{10})v_i(\tau,z)$ $(i=x,z)$, in the HOCLC cell, at the final stage of the relaxation process are equal to 0.2 ($\sim$0.3 μm/s) and 0.7 ($\sim$1 μm/s), for vertical and horizontal components, respectively [see Figs. 1(a) and 1(c)], at $\Delta\chi=0.0162$. It should be pointed out that the dimensionless temperature field $\chi(\tau,z)$ relaxes to its equilibrium distribution $\chi_{\rm eq}(z)$ across the LC cell during the time term $\Delta\tau\sim 10^{-3}$ ($\sim$1 s), which means that the temperature field relaxes much faster, approximately one order of magnitude, then relaxes both the dimensionless velocity components and the director. The character of the relaxation process of the dimensionless velocity fields $u(\tau,z)$ and $w(\tau,z)$ with changing τ, before getting to the equilibrium distributions $u_{\rm eq}(z)$ and $w_{\rm eq}(z)$, across the LC cell, is changed with changing of the temperature gradient direction [see Figs. 3(a) and 3(c)]. According to our calculations, when the temperature gradient was directed from the bottom to the top surfaces ($\chi_2>\chi_1$), one has arrived to the picture where the LC fluid settles down to the stationary flow regimes in the negative direction, both for the horizontal and vertical components of the hydrodynamic flow [see Figs. 1(a) and 1(c)], whereas in the case when the temperature gradient was directed from the top to the bottom surfaces ($\chi_1>\chi_2$), one has arrived at the picture where the LC fluid settles down to the stationary flow regimes in the positive direction, both for the horizontal and vertical components of the hydrodynamic flow [see Figs. 3(a) and 3(c)]. In the last case, the maximum of the absolute magnitude of the dimensionless velocity $u(\tau,z)=(\gamma_{10}d/K_{10})v_x(\tau,z)$, in the HOCLC cell, at the final stage of the relaxation process is equal to 0.3 ($\sim$0.4 μm/s) [Fig. 3(a)], whereas the maximum of $w(\tau,z)$ is equal to 0.1 ($\sim$0.14 μm/s) [Fig. 3(c)], at $\Delta\chi=0.0162$, respectively. At that, the dimensionless relaxation time is $\tau_R\sim 0.5$ ($\sim$36 s). According to our calculations the relaxation of the director $\hat{\mathbf{n}}$ to its equilibrium orientation $\hat{\mathbf{n}}_{\rm eq}$, which is described by the polar angle $\theta(\tau,z)$ from the initial condition $\theta(\tau=0,0.0<z\leqslant 1.0)=\frac{\pi}{2}$ to $\theta_{\rm eq}$, at different times ($\tau(1)=0.04$ [curve (1)], $\tau(2)=0.08$ [curve (2)], …, $\tau(13)=\tau_R=0.5$ [curve (13)]), is shown in Fig. 3(b). In that case the sample is heated from below with the dimensionless temperature difference $\Delta\chi=0.0162$ ($\sim$5 K). The relaxation processes of the dimensionless temperature $\chi(\tau,z)$ and density $\rho(\tau,z)$ to their equilibrium distributions $\chi_{\rm eq}(z)$ and $\rho_{\rm eq}(z)$ across the LC cell, are also characterized practically the linear behavior [see Figs. 4(a) and 4(b)] of these quantities. In the case when the director is weakly anchored to the upper restricted surface ($z=1$), the effect of the dimensionless strength anchoring $(Ad/K_{30})\Delta\theta$ on the magnitudes, both $u(\tau,z)$ and $w(\tau,z)$, are negligibly small and practically does not change the equilibrium distributions of these velocities between two bounding surfaces. Our calculations also show that the relaxation time τ_R of the velocity field $u(\tau,z)$ to $u_{\rm eq}(z)$ across the HOCLC cell increase up to 15%, in the case of the weak anchoring $[(Ad/K_{30})\Delta\theta=0.1]$ on the upper bounding surface in comparison with the case of the strong anchoring. Such behavior of $u(\tau,z)$ shows that the director field, in the vicinity of the upper restricted surface, has a weak influence on the velocity field. Indeed, due to the decrease of interactions between the solid wall and the LC phase, in the case of the weak anchoring to the upper boundary, the LC system spend a little bit more time for relaxation to its equilibrium distribution across the LC sample than in the case of the strong anchoring. So,

the strong anchoring may be expected to produce a greater rigidity of the LC sample near the solid wall. Note, that in both last cases, the temperature gradient was directed from the top to the bottom of the bounding surfaces.

IV. ORIENTATIONAL RELAXATION THE TOTAL STRESS TENSOR COMPONENTS

Our attention now turns to the stress tensor σ_{ij} which also can be obtained directly from the Rayleigh dissipation function $\mathcal{R}(t,z)=(K_{10}^2/\gamma_{10}d^4)\mathcal{R}(\tau,z)$ as [9,24,25]

$$\sigma_{zx}(\tau) = \partial\mathcal{R}(\tau)/\partial u_z \tag{19}$$

and

$$\sigma_{zz}^{v}(\tau) = \partial\mathcal{R}(\tau)/\partial w_z, \tag{20}$$

where it is taken into account that $\sigma_{zx}=\sigma_{zx}^{v}+\sigma_{zx}^{e}$ and $\sigma_{zx}^{e}=0$. Having obtained σ_{zx}, and using the relation $\sigma_{zx}(\tau)-\sigma_{xz}(\tau)=\partial\mathcal{R}(\tau)/\partial\theta_\tau$, one can calculate the dimensionless stress tensor component σ_{xz}, which takes the form

$$\sigma_{xz}(\tau) = \sigma_{zx}(\tau) - [\mathcal{G}(\theta)\theta_z]_z + \frac{1}{2}\mathcal{G}_\theta(\theta)\theta_z^2. \tag{21}$$

In the case of planar geometry, the form of σ_{zz}^{v} is given by

$$\sigma_{xx}^{v}(\tau,z) = \sigma_{zz}^{v}(\tau,z), \tag{22}$$

whereas the full forms of σ_{zz} and σ_{xx} are given by

$$\sigma_{zz}(\tau,z) = \sigma_{zz}^{v}(\tau,z) + \sigma_{zz}^{e}(\tau,z) = \sigma_{zz}^{v}(\tau,z) - \mathcal{G}(\theta)\theta_z^2 \tag{23}$$

and

$$\sigma_{xx}(\tau,z) = \sigma_{zz}^{v}(\tau,z) + \sigma_{xx}^{e}(\tau,z) = \sigma_{zz}^{v}(\tau,z), \tag{24}$$

respectively. Here it is taken into account that $\sigma_{xx}^{e}=0$ (see the Appendix). Calculations of the evolution of the dimensionless stress tensor components $\sigma_{xx}(\tau,z)$, $\sigma_{xz}(\tau,z)$, $\sigma_{zx}(\tau,z)$, and $\sigma_{zz}(\tau,z)$ vs distance z away from the cooler ($\chi_{z=0}=\chi_1=0.97$) lower surface directed to the warmer ($\chi_{z=1}=\chi_1+\Delta\chi$) upper one, and from the warmer ($\chi_{z=0}=\chi_1+\Delta\chi$) lower surface directed to the cooler ($\chi_{z=1}=\chi_1=0.97$) upper one, in the HOCLC cell, using Eqs. (2), (8)–(10), and (18), with the boundary conditions (12) and (13), at different times, are shown in Figs. 5 and 6, respectively. The relaxation of $\sigma_{ij}(\tau,z)$ $(i,j=x,z)$ to its equilibrium values $\sigma_{ij}^{eq}(z)$, at the final stage of the relaxation process, at different times ($\tau(1)=0.1$ [curve (1)], $\tau(2)=0.2$ [curve (2)], …, $\tau(5)=\tau_R=0.5$ [curve (5)]), when the sample is heated from above with the dimensionless temperature difference $\Delta\chi=0.0162$ (~5 K), is shown in Fig. 5. The normal $\sigma_{xx}(\tau,z)$ [Fig. 5(a)] and shear $\sigma_{xz}(\tau,z)$ [Fig. 5(b)] components of the stress tensor $\sigma_{ij}(\tau,z)$ demonstrate a strong increase of the absolute magnitude of these quantities in the vicinity of the bounding surfaces $z=0$ and $z=1$, and the decrease of $|\sigma_{xi}(\tau,z)|$ $(i=x,z)$ to zero, in the middle part of the HOCLC cell. Calculation also shows that the relaxation processes both the dimensionless shear $\sigma_{zx}(\tau)$ and normal $\sigma_{zz}(\tau)$ stress tensor components are characterized by monotonic decreasing of these quantities across the LC sample with growth of time. At that the values of σ_{zz}

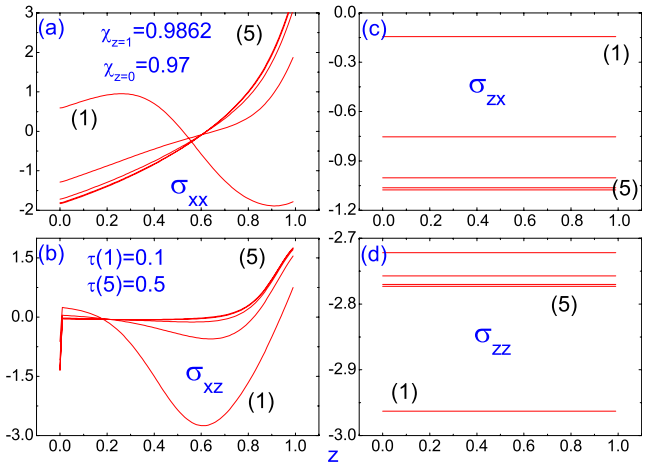

FIG. 5. (Color online) The dimensionless stress tensor components $\sigma_{xx}(\tau,z)$ (a), $\sigma_{xz}(\tau,z)$ (b), $\sigma_{zx}(\tau,z)$ (c), and $\sigma_{zz}(\tau,z)$ (d), vs distance z away from the lower cooler ($\chi_{z=0}=\chi_1=0.97$) to the upper warmer ($\chi_{z=1}=\chi_1+\Delta\chi$) upper bounding surfaces in the HOCLC cell, at different times $\tau(1)=0.1$ (curve (1) and $\tau(k)=(k/5)\tau_R$, $k=1,\ldots,5$, whose values increase from curve (1) to curve (5). Here $\Delta\chi=0.0162$ and $\tau_R\sim0.5$, respectively.

and σ_{zx} are negative, with growth of time τ. Note that both $\sigma_{zx}(\tau)$ and $\sigma_{zz}(\tau)$, according to Eqs. (15) and (16), are only time-dependent functions. When the temperature gradient directed from the cooler upper ($\chi_2=0.97$) to the warmer lower ($\chi_1=\chi_2+\Delta\chi$) restricted surface, the relaxation of $\sigma_{ij}(\tau,z)$ $(i,j=x,z)$ to its equilibrium value $\sigma_{ij}^{eq}(z)$, at different times ($\tau(1)=0.1$ [curve(1)], $\tau(2)=0.2$ [curve(2)], …, $\tau(5)=\tau_R=0.5$ [curve(5)]), is shown in Fig. 6. Here the sample is heated with the dimensionless temperature difference $\Delta\chi=0.0162$ (~5 K). In that case the normal $\sigma_{xx}(\tau,z)$ [Fig. 6(a)] and shear $\sigma_{xz}(\tau,z)$ [Fig. 6(b)] components demonstrate, as in the previous case [Figs. 5(a) and 5(b)], a strong decrease of the absolute magnitude of these quantities in the vicinity of the bounding surfaces $z=0$ and $z=1$, and the decrease of $|\sigma_{xi}(\tau,z)|$ $(i=x,z)$ to zero, in the middle part of the HOCLC

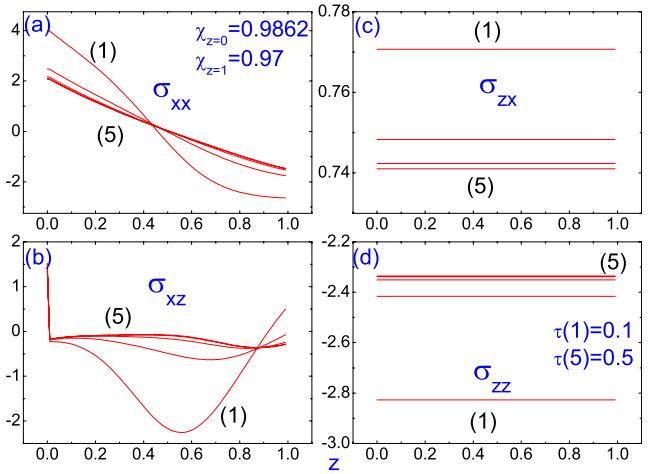

FIG. 6. (Color online) The same as in Fig. 5, but the temperature gradient directed from the upper cooler ($\chi_{z=1}=\chi_2=0.97$) to the lower warmer ($\chi_{z=0}=\chi_2+\Delta\chi$) bounding surfaces in the HOCLC cell.

cell. But in the last case [Figs. 6(a) and 6(b)], in the vicinity of the warmer lower restricted surface ($z=0$), the normal σ_{xx} and shear σ_{xz} components are both directed in the positive directions, whereas in the previous case [Figs. 5(a) and 5(b)], these quantities, in the vicinity of the cooler lower restricted surface, are directed in the negative direction, respectively. The character of relaxation process of $\sigma_{xi}(\tau,z)$ $(i=x,z)$ is also changed with changing of the temperature gradient direction [see, Figs. 5(a) and 5(b) and Figs. 6(a) and 6(b), respectively], in the vicinity of the upper restricted surface. The maximum of the absolute magnitude of the dimensional stress tensor components $\bar{\sigma}_{ij}=(K_{10}/d^2)\sigma_{ij}$ $(i,j=x,z)$, at the final stage of the relaxation process has been found ~ 0.004 Pa, for the normal component σ_{xx} in the vicinity of the warmer lower restricted surface. Such behavior of the equilibrium distribution of $\sigma_{ij}(z)$ $(i,j=x,z)$ shows that the direction and magnitude of the hydrodynamic flow has a strong influence on the character of the relaxation process of the stress tensor components σ_{xx}, σ_{xz}, σ_{zx}, and σ_{zz}, and that behavior both qualitatively and quantitatively differ than one corresponding to confined incompressible LC film under influence of the vertical temperature gradient [9].

V. CONCLUSION

In summary, we have investigated the relaxation of director $\hat{\mathbf{n}}(t,\mathbf{r})$, velocity $\mathbf{v}(t,\mathbf{r})$, density $\rho(t,\mathbf{r})$, and the stress tensor components $\sigma_{ij}(t,\mathbf{r})$ $(i,j=x,z)$ in the HOCLC cell to their equilibrium values, under influence of the temperature gradient directed normal to the bounding surfaces. Our calculations, based upon the classical Leslie-Ericksen theory, shows that the HOCLC material under influence of the temperature gradient, settles down to a stationary flow regime with the horizontal u and vertical w components. It has been also shown that the magnitudes of these velocities u and w are proportional to the tangential and normal components of the stress tensor components σ_{zx}^{tm} and σ_{zz}^{tm}, and the direction of $\mathbf{v}=u\hat{\mathbf{i}}+w\hat{\mathbf{k}}$ influence the direction of heat flow. At that, the character of the preferred anchoring of the director to the bounding surfaces, practically, does not influence on the magnitudes of these velocities. Notes, that in the case of the hybrid-oriented incompressible LC cell, where, due to an incompressibility condition $\nabla\cdot\mathbf{v}=0$, there is only one nonzero component of the vector $\mathbf{v}$, viz., $\mathbf{v}=v_x\hat{\mathbf{i}}=u\hat{\mathbf{i}}$, the character of the preferred anchoring of the director to the restricted surfaces has a strong effect [9] on the magnitude of $u(z)$, excited by the heat flow. In the case of the compressible fluid, that horizontal stationary flow $u(z)$ is directed in the opposite direction, approximately, in one order of the magnitude less, than one in the case of the incompressible fluid. The maximums of the absolute magnitudes of the dimensionless horizontal velocity $v_x(\tau,z)=(\gamma_{10}d/K_{10})v_x(\tau,z)$ $(i=x,z)$, in the HOCLC cell, at the final stage of the relaxation process, approximately, one order of the magnitude less, than one in the case of the incompressible fluid. Such redistribution of the stationary hydrodynamic flow in the HOCLC fluid leads to differ redistribution, than one in the case of the incompressible fluid, of the stress tensor components. So, the maximum of the absolute magnitude of the dimension stress tensor for the normal component $\bar{\sigma}_{zz}=(K_{10}/d^2)\sigma_{zz}$, at the final stage of the relaxation process, has been found to be ~ 0.002 Pa, one order of magnitude less than in the case of the incompressible fluid [9].

We believe that the present investigation can shed some light on the problem of the reorientation process in the HOCLC cell under influence of the vertical temperature gradient. We also believe that the paper shows not only some useful routes for estimating the relaxation times, but also analyzing the remaining problems associated with LC device stability, efficiency, and lifetime.

APPENDIX: RAYLEIGH DISSIPATION FUNCTION AND THE STRESS TENSOR COMPONENTS

In the case of compressible nematic fluid $\partial_t\rho+\nabla\cdot(\rho\mathbf{v})=0$, it is convenient to rewrite the Rayleigh dissipation function $\mathcal{R}(t,z)$ in the form with and without accounting for the compressible term as [24]

$$\mathcal{R}(t,z)=\mathcal{R}_1(t,z)+\mathcal{R}_2(t,z), \tag{A1}$$

where $\mathcal{R}_1(t,z)=(\boldsymbol{\sigma}+\frac{\partial W_F}{\partial\nabla\hat{\mathbf{n}}}\cdot\hat{\mathbf{n}}\nabla):\mathbf{v}\nabla=\sigma^v:\mathbf{v}\nabla$ and $\mathcal{R}_2(t,z)=(\boldsymbol{\sigma}^m-\hat{\mathbf{n}}\times\frac{\partial W_F}{\partial\hat{\mathbf{n}}\nabla}):\vec{\omega}\nabla-\vec{\omega}\cdot\mathcal{E}:(\sigma+\frac{\partial W_F}{\partial\nabla\hat{\mathbf{n}}}\cdot\hat{\mathbf{n}}\nabla)=\sigma^{mv}:\vec{\omega}\nabla-\vec{\omega}\cdot\mathcal{E}:\sigma^v$, respectively. Here $\mathbf{v}$ and $\vec{\omega}$ are the linear and angular velocities, $\nabla\mathbf{v}$ and $\nabla\vec{\omega}$ are the gradients of these fields, $\sigma=\sigma^v+\sigma^e$ and $\sigma^m=\sigma^{mv}+\sigma^{me}$ are the stress and the momentum stress tensors, $\mathcal{E}$ is the Levi-Civita tensor, $W_F=\frac{1}{2}[K_1n_{z,z}^2+K_3n_{x,z}^2]$ is the Frank elastic energy, $\hat{\mathbf{n}}=(n_x,0,n_z)$, K_1 and K_3 are the Frank elastic constants, $\sigma^v=\frac{\partial\mathcal{R}}{\partial\nabla\mathbf{v}}$, $\sigma^e=-\frac{\partial W_F}{\partial\nabla\hat{\mathbf{n}}}\cdot\hat{\mathbf{n}}\nabla$, $\sigma^{mv}=\frac{\partial\mathcal{R}}{\partial\nabla\vec{\omega}}$, and $\sigma^{me}=\hat{\mathbf{n}}\times\frac{\partial W_F}{\partial\hat{\mathbf{n}}\nabla}$ are the viscous and elastic contributions to the total stress σ and momentum stress σ^m tensors, respectively. We use invariant, multiple dot convention: $\mathbf{a}\cdot\mathbf{b}=a_ib_i$, $\mathbf{A}\cdot\mathbf{B}=A_{ik}B_{kj}$, and $\mathbf{A}:\mathbf{B}=A_{ik}B_{ki}$, where repeated Cartesian indices are summed. By means of decomposition of the tensors on the spherical, symmetric and asymmetric deviators one can rewrite the last two tensors and gradients $\mathbf{v}\nabla$ and $\vec{\omega}\nabla$ in the form [24] $\sigma^v=\sigma_0^v\mathcal{I}+\sigma_s^v+\sigma_a^v$, $\sigma^{mv}=\sigma_0^{mv}\mathcal{I}+\sigma_s^{mv}+\sigma_a^{mv}$, $\mathbf{v}\nabla=v_0\mathcal{I}+\mathbf{v}\nabla_s+\mathbf{v}\nabla_a$, and $\vec{\omega}\nabla=\omega_0\mathcal{I}+\vec{\omega}\nabla_s+\vec{\omega}\nabla_a$, respectively. Here $\mathcal{I}$ is the unit tensor. Now the full dissipation function $\mathcal{R}$ can be written as

$$\mathcal{R}(t,z)=\sigma_0^vv_0\mathcal{I}:\mathcal{I}+\sigma_s^v:\mathbf{v}\nabla_s+\sigma_a^v:\mathbf{v}\nabla_a+\sigma_0^{mv}\omega_0\mathcal{I}:\mathcal{I}+\sigma_s^{mv}:\vec{\omega}\nabla_s+\sigma_a^{mv}:\vec{\omega}\nabla_a. \tag{A2}$$

In the following, one deals with the complicated flow $\mathbf{v}=(u,0,w)$ excited by the temperature gradient and the director reorientation with four components of the viscous stress tensor σ_{xx}^v, σ_{xz}^v, σ_{zx}^v, and σ_{zz}^v, which are connected each other by relations $2\sigma_0^v=\sigma_{xx}^v+\sigma_{zz}^v$, $2v_0=w_z$, and $2\sigma_0^v=\partial\mathcal{R}/\partial v_0$, respectively. Taking into account the last two equations (A1) and (A2), the equations for the tensor components σ_{xx}^v and σ_{zz}^v can be written in the form

$$\sigma^v_{zz} + \sigma^v_{xx} = 2\frac{\partial \mathcal{R}(t,z)}{\partial w_z}, \tag{A3}$$

$$\sigma^v_{zz} = \frac{\partial \mathcal{R}(t,z)}{\partial w_z}. \tag{A4}$$

The last system of equations (A3) and (A4) has a solution

$$\sigma^v_{zz} = \sigma^v_{xx}.$$

Note that the compressible part of $\mathcal{R}(t,z)$ can be decomposed as $\frac{1}{2}P\nabla\cdot\mathbf{v}+\frac{1}{2}\sigma^v_s:(\nabla\mathbf{v}+\mathbf{v}\nabla)+\frac{1}{2}\sigma^v_a:(\nabla\mathbf{v}-\mathbf{v}\nabla)$, where σ^v_s and σ^v_a are symmetric and asymmetic deviators of the tensor σ^v, whereas $P=\sigma^v:\mathcal{I}=\sigma^v_{xx}+\sigma^v_{zz}$ is the viscous contribution to the total pressure $\bar{P}$. The elastic contribution to $\bar{P}$ is equal to $P^e=\sigma^e:\mathcal{I}=\sigma^e_{xx}+\sigma^e_{zz}=-2W_F$. So, the total dimensionless pressure is given by $\bar{P}=2(\sigma^v_{zz}-W_F)$.

[1] P. G. de Gennes and J. Prost, *The Physics of Liquid Crystals*, 2nd ed. (Oxford University Press, Oxford, 1995).
[2] O. Lehmann, Ann. Phys. **4**, 649 (1900).
[3] F. M. Leslie, Proc. R. Soc. London, Ser. A **307**, 359 (1968).
[4] N. Eber and I. Janossy, Mol. Cryst. Liq. Cryst. Lett. **72**, 233 (1982).
[5] R. S. Akopyan and B. Ya. Zeldovich, JETP **60**, 953 (1984).
[6] H. R. Brand and H. Pleiner, Phys. Rev. A **37**, 2736 (1988).
[7] R. S. Akopyan, R. B. Alaverdian, E. A. Santrosian, and Y. S. Chilingarian, J. Appl. Phys. **90**, 3371 (2001).
[8] R. S. Hakobyan, G. L. Yesayan, and B. Ya. Zeldovich, Phys. Rev. E **73**, 061707 (2006).
[9] A. V. Zakharov and A. A. Vakulenko, J. Chem. Phys. **127**, 084907 (2007).
[10] A. V. Zakharov, A. A. Vakulenko, and S. Romano, J. Chem. Phys. **128**, 074905 (2008).
[11] A. Dequidt and P. Oswald, Europhys. Lett. **80**, 26001 (2007).
[12] J. L. Ericksen, Arch. Ration. Mech. Anal. **4**, 231 (1960).
[13] F. M. Leslie, Arch. Ration. Mech. Anal. **28**, 265 (1968).
[14] L. D. Landau and E. M. Lifshitz, *Fluid Mechanics* (Pergamon, Oxford, 1987).
[15] M. C. Cross and P. C. Hohenberg, Rev. Mod. Phys. **65**, 851 (1993).
[16] R. Graham, Phys. Rev. A **10**, 1762 (1974).
[17] N. V. Madhusudana and R. P. Pratibha, Mol. Cryst. Liq. Cryst. **89**, 249 (1982).
[18] A. G. Chmielewski, Mol. Cryst. Liq. Cryst. **132**, 339 (1986).
[19] L. M. Blinov, A. Yu. Kabaenkov, and A. A. Sonin, Liq. Cryst. **5**, 645 (1989).
[20] P. Jamee, G. Pitsi, and J. Thoen, Phys. Rev. E **66**, 021707 (2002).
[21] M. Marinelli, A. K. Ghosh, and F. Mercuri, Phys. Rev. E **63**, 061713 (2001).
[22] W. Wedler, *Physical Properties of Liquid Crystals*, edited by D. Demus, J. Goodby, G. W. Gray, H.-W. Spiess, and W. Vill (Wiley-VCH, Weinheim, 1999).
[23] I. S. Berezin and N. P. Zhidkov, *Computing Methods*, 4th ed. (Pergamon Press, Oxford, 1965).
[24] I. W. Stewart, *The Static and Dynamic Continuum Theory of Liquid Crystals* (Taylor and Francis, London, 2004).
[25] S. R. de Groot and P. Mazur, *Non-equilibrium Thermodynamics* (North-Holland, Amsterdam, 1962).